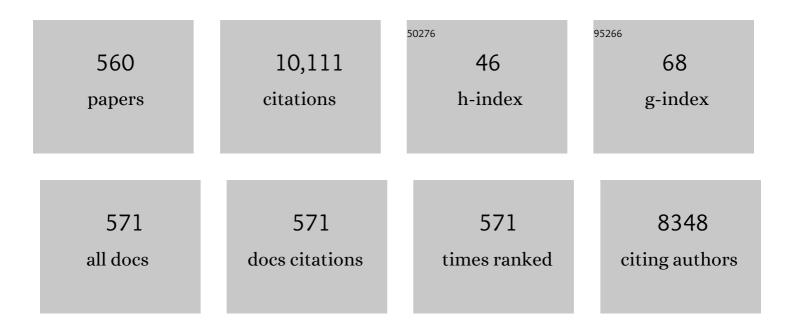
List of Publications by Year in descending order

Source: https://exaly.com/author-pdf/8963724/publications.pdf Version: 2024-02-01



MALIDIZIO FEDDADI

#	Article	IF	CITATIONS
1	Spherical whisperingâ€galleryâ€mode microresonators. Laser and Photonics Reviews, 2010, 4, 457-482.	8.7	384
2	Fabrication and characterization of nanoscale, Er3+-doped, ultratransparent oxy-fluoride glass ceramics. Applied Physics Letters, 2002, 81, 1937-1939.	3.3	213
3	Luminescence of Eu ³⁺ ions during thermal densification of SiO ₂ gel. Journal of Materials Research, 1992, 7, 745-753.	2.6	144
4	Erbium-doped tellurite glasses with high quantum efficiency and broadband stimulated emission cross section at 1.5 μm. Optical Materials, 2003, 21, 743-748.	3.6	139
5	Clustering of rare earth in glasses, aluminum effect: experiments and modeling. Journal of Non-Crystalline Solids, 2004, 348, 44-50.	3.1	122
6	Mechanisms of Ag to Er energy transfer in silicate glasses: A photoluminescence study. Physical Review B, 2007, 75, .	3.2	121
7	Erbium-activated HfO2-based waveguides for photonics. Optical Materials, 2004, 25, 131-139.	3.6	116
8	Sol-gel Er-doped SiO2–HfO2 planar waveguides: A viable system for 1.5 μm application. Applied Physics Letters, 2002, 81, 28-30.	3.3	107
9	Spectroscopic investigation of zinc borate glasses doped with trivalent europium ions. Journal of Non-Crystalline Solids, 1996, 201, 211-221.	3.1	106
10	Low optical loss planar waveguides prepared in an organic–inorganic hybrid system. Applied Physics Letters, 2000, 77, 3502-3504.	3.3	104
11	Diamond photonics platform enabled by femtosecond laser writing. Scientific Reports, 2016, 6, 35566.	3.3	96
12	Optical investigation ofEu3+in a sodium borosilicate glass: Evidence for two different site distributions. Physical Review B, 1996, 53, 6225-6234.	3.2	80
13	Luminescence and Amplified Stimulated Emission in CdSe-ZnS-Nanocrystal-Doped TiO2 and ZrO2 Waveguides. Advanced Functional Materials, 2007, 17, 1654-1662.	14.9	77
14	Optical spectroscopy of zinc borate glass activated by Pr3+ ions. Journal of Non-Crystalline Solids, 1998, 231, 178-188.	3.1	74
15	Coenzyme A corrects pathological defects in human neurons of <scp>PANK</scp> 2â€associated neurodegeneration. EMBO Molecular Medicine, 2016, 8, 1197-1211.	6.9	74
16	Low wavenumber Raman scattering of nanoparticles and nanocomposite materials. Journal of Raman Spectroscopy, 2007, 38, 647-659.	2.5	73
17	Design of photonic structures by sol–gel-derived silica nanospheres. Journal of Non-Crystalline Solids, 2007, 353, 674-678.	3.1	69
18	Enhanced fluorescence from Eu3+ in low-loss silica glass-ceramic waveguides with high SnO2 content. Applied Physics Letters, 2008, 93, .	3.3	69

#	Article	IF	CITATIONS
19	Dysprosium-Doped Chalcogenide Master Oscillator Power Amplifier (MOPA) for Mid-IR Emission. Journal of Lightwave Technology, 2017, 35, 265-273.	4.6	69
20	High quality factor 1-D Er^3+-activated dielectric microcavity fabricated by RF-sputtering. Optics Express, 2012, 20, 21214.	3.4	64
21	Investigation on the Electronic and Optical Properties of Short Oxidized Multiwalled Carbon Nanotubes. Journal of Physical Chemistry C, 2010, 114, 11068-11073.	3.1	63
22	Design of an Efficient Pumping Scheme for Mid-IR Dy ³⁺ :Ga ₅ Ge ₂₀ Sb ₁₀ S ₆₅ PCF Fiber Laser. IEEE Photonics Technology Letters, 2016, 28, 1984-1987.	2.5	63
23	Detection and size determination of Ag nanoclusters in ionâ€exchanged sodaâ€lime glasses by waveguided Raman spectroscopy. Journal of Applied Physics, 1996, 79, 2055-2059.	2.5	62
24	Active optical waveguides based on Er- and Er/Yb-doped silicate glasses. Journal of Non-Crystalline Solids, 2001, 284, 223-229.	3.1	59
25	Self-absorption and radiation trapping in Er 3 + -doped TeO 2 -based glasses. Europhysics Letters, 2005, 71, 394-399.	2.0	59
26	Integrated waveguides and deterministically positioned nitrogen vacancy centers in diamond created by femtosecond laser writing. Optics Letters, 2018, 43, 3586.	3.3	59
27	Granulosa cell and oocyte mitochondrial abnormalities in a mouse model of fragile X primary ovarian insufficiency. Molecular Human Reproduction, 2016, 22, 384-396.	2.8	58
28	Sol–gel-derived Er-activated SiO2–HfO2 planar waveguides for 1.5μm application. Journal of Non-Crystalline Solids, 2004, 345-346, 580-584.	3.1	56
29	Assessment of spectroscopic properties of erbium ions in a soda-lime silicate glass after silver–sodium exchange. Optical Materials, 2005, 27, 1743-1747.	3.6	56
30	Erbium-activated silica xerogels: spectroscopic and optical properties. Journal of Non-Crystalline Solids, 2001, 280, 261-268.	3.1	55
31	Structural and near-infra red luminescence properties of Nd-doped TiO2 films deposited by RF sputtering. Journal of Materials Chemistry, 2012, 22, 22424.	6.7	55
32	Terbium(III) doped silica-xerogels: effect of aluminium(III) co-doping. Journal of Non-Crystalline Solids, 1999, 245, 115-121.	3.1	54
33	Sol–gel-derived photonic structures: fabrication, assessment, and application. Journal of Sol-Gel Science and Technology, 2011, 60, 408-425.	2.4	54
34	Structural and functional brain signatures of C9orf72 in motor neuron disease. Neurobiology of Aging, 2017, 57, 206-219.	3.1	54
35	Analysis of Clinically Relevant Single-Nucleotide Polymorphisms by Use of Microelectronic Array Technology. Clinical Chemistry, 2002, 48, 2124-2130.	3.2	53
36	Infrared-to-visible CW frequency upconversion in erbium activated silica–hafnia waveguides prepared by sol–gel route. Journal of Non-Crystalline Solids, 2003, 322, 306-310.	3.1	53

#	Article	IF	CITATIONS
37	Tb3+/Yb3+ codoped silica–hafnia glass and glass–ceramic waveguides to improve the efficiency of photovoltaic solar cells. Optical Materials, 2016, 52, 62-68.	3.6	53
38	Pulsed laser deposition of active waveguides. Thin Solid Films, 2003, 433, 39-44.	1.8	52
39	Investigation of the role of silver on spectroscopic features of Er3+-activated Ag-exchanged silicate and phosphate glasses. Journal of Non-Crystalline Solids, 2005, 351, 1738-1742.	3.1	52
40	Low-loss optical Er3+-activated glass-ceramics planar waveguides fabricated by bottom-up approach. Applied Physics Letters, 2007, 91, .	3.3	50
41	Erbium activated HfO2 based glass–ceramics waveguides for photonics. Journal of Non-Crystalline Solids, 2007, 353, 494-497.	3.1	50
42	Quantum Confinement and Matrix Effects in Silver-Exchanged Soda Lime Glasses. Journal of Physical Chemistry C, 2009, 113, 4445-4450.	3.1	50
43	Exome sequencing and pathway analysis for identification of genetic variability relevant for bronchopulmonary dysplasia (BPD) in preterm newborns: A pilot study. Clinica Chimica Acta, 2015, 451, 39-45.	1.1	49
44	Visible to NIR downconversion process in Tb3+-Yb3+ codoped silica-hafnia glass and glass-ceramic sol-gel waveguides for solar cells. Journal of Luminescence, 2018, 193, 44-50.	3.1	49
45	ADCY10 frameshift variant leading to severe recessive asthenozoospermia and segregating with absorptive hypercalciuria. Human Reproduction, 2019, 34, 1155-1164.	0.9	49
46	Glassâ€Ceramic Materials for Guidedâ€Wave Optics. International Journal of Applied Glass Science, 2015, 6, 240-248.	2.0	48
47	Investigations of the effects of the growth of SnO2 nanoparticles on the structural properties of glass–ceramic planar waveguides using Raman and FTIR spectroscopies. Journal of Molecular Structure, 2010, 976, 314-319.	3.6	47
48	Tb3+/Yb3+ co-activated Silica-Hafnia glass ceramic waveguides. Optical Materials, 2010, 33, 227-230.	3.6	47
49	Incorporation of a highly luminescent semiconductor quantum dot in ZrO2–SiO2hybrid sol–gel glass film. Journal of Materials Chemistry, 2004, 14, 1112-1116.	6.7	46
50	Effects of <scp><scp>Tm</scp></scp> ³⁺ Additions on the Crystallization of <scp><scp>LaF</scp></scp> 3 Nanocrystals in Oxyfluoride Glasses: Optical Characterization and Upâ€Conversion. Journal of the American Ceramic Society, 2013, 96, 447-457.	3.8	46
51	Stem Cell Modeling of Neuroferritinopathy Reveals Iron as a Determinant of Senescence and Ferroptosis during Neuronal Aging. Stem Cell Reports, 2019, 13, 832-846.	4.8	46
52	Sol-Gel Based Vertical Optical Microcavities with Quantum Dot Defect Layers. Advanced Functional Materials, 2008, 18, 3772-3779.	14.9	45
53	Optical field enhanced nonlinear absorption and optical limiting properties of 1-D dielectric photonic crystal with ZnO defect. Optical Materials, 2015, 50, 229-233.	3.6	45
54	β-Thalassemia Microelectronic Chip: A Fast and Accurate Method for Mutation Detection. Clinical Chemistry, 2004, 50, 73-79.	3.2	44

#	Article	IF	CITATIONS
55	Optical spectroscopy of TeO2–GeO2 glasses activated with Er3+ and Tm3+ ions. Journal of Non-Crystalline Solids, 2005, 351, 1759-1763.	3.1	43
56	An alternative method to obtain direct opal photonic crystal structures. Journal of Non-Crystalline Solids, 2009, 355, 1167-1170.	3.1	43
57	Thermal stability and spectroscopic properties of erbium-doped niobic-tungsten–tellurite glasses for laser and amplifier devices. Journal of Luminescence, 2012, 132, 1265-1269.	3.1	43
58	X-linked Parkinsonism with Intellectual Disability caused by novel mutations and somatic mosaicism in RAB39B gene. Parkinsonism and Related Disorders, 2017, 44, 142-146.	2.2	43
59	Titania-based organic–inorganic hybrid planar waveguides. Journal of Alloys and Compounds, 2002, 344, 221-225.	5.5	42
60	Up- and down-conversion in Yb3+–Pr3+ co-doped fluoride glasses and glass ceramics. Journal of Non-Crystalline Solids, 2013, 377, 105-109.	3.1	42
61	Disorder in Photonic Structures Induced by Random Layer Thickness. Science of Advanced Materials, 2015, 7, 1207-1212.	0.7	42
62	Effect of Genotypic Resistance on the Virological Response to Highly Active Antiretroviral Therapy in Cerebrospinal Fluid. AIDS Research and Human Retroviruses, 2001, 17, 377-383.	1.1	41
63	Erbium-Activated Silica-Titania Planar Waveguides. Journal of Sol-Gel Science and Technology, 2003, 26, 1033-1036.	2.4	41
64	Tm3+-activated transparent oxy-fluoride glass–ceramics: structural and spectroscopic properties. Journal of Non-Crystalline Solids, 2004, 345-346, 354-358.	3.1	41
65	High quality factor Er3+-activated dielectric microcavity fabricated by rf sputtering. Applied Physics Letters, 2006, 89, 171910.	3.3	41
66	Preparation of silver nanoparticles in silica films by combined thermal and electron-beam deposition. Journal of Non-Crystalline Solids, 1995, 191, 101-106.	3.1	40
67	Preparation of SiO ₂ â€"GeO ₂ : Eu ³⁺ planar waveguides and characterization by waveguide Raman and luminescence spectroscopies. The Philosophical Magazine: Physics of Condensed Matter B, Statistical Mechanics, Electronic, Optical and Magnetic Properties, 1998. 77. 363-372.	0.6	40
68	Title is missing!. Optical and Quantum Electronics, 2002, 34, 1151-1166.	3.3	40
69	Nucleation of Titania Nanocrystals in Silica Titania Waveguides. Journal of Sol-Gel Science and Technology, 2003, 26, 241-244.	2.4	40
70	Tin-dioxide nanocrystals as Er 3+ luminescence sensitizers: Formation of glass-ceramic thin films and their characterization. Optical Materials, 2017, 63, 95-100.	3.6	40
71	Femtosecond laser written photonic and microfluidic circuits in diamond. JPhys Photonics, 2019, 1, 022001.	4.6	40
72	Peptide-nucleic acid-mediated enriched polymerase chain reaction as a key point for non-invasive prenatal diagnosis of Â-thalassemia. Haematologica, 2008, 93, 610-614.	3.5	39

#	Article	IF	CITATIONS
73	Microelectronic DNA chip for hereditary hyperferritinemia cataract syndrome, a model for large-scale analysis of disorders of iron metabolism. Human Mutation, 2006, 27, 201-208.	2.5	38
74	Er3+ ion dispersion in tellurium oxychloride glasses. Optical Materials, 2007, 29, 503-509.	3.6	38
75	Monolithic rare-earth doped sol-gel tapered rib waveguide laser. Applied Physics Letters, 2008, 92, 221104.	3.3	38
76	Spectroscopy of trivalent europium in gel-derived silica glasses. The Philosophical Magazine: Physics of Condensed Matter B, Statistical Mechanics, Electronic, Optical and Magnetic Properties, 1992, 65, 251-260.	0.6	37
77	Nucleation of Ga2O3 nanocrystals in the K2O–Ga2O3–SiO2 glass system. Journal of Applied Physics, 2001, 90, 2522-2527.	2.5	37
78	Erbium doped fluoride glass–ceramics waveguides fabricated by PVD. Journal of Non-Crystalline Solids, 2008, 354, 3586-3591.	3.1	37
79	Rare-earth-activated glass–ceramic waveguides. Optical Materials, 2010, 32, 1644-1647.	3.6	37
80	Integrated PCR amplification and detection processes on a Lab-on-Chip platform: a new advanced solution for molecular diagnostics. Clinical Chemistry and Laboratory Medicine, 2010, 48, 329-336.	2.3	37
81	The 1-in- <i>X</i> Effect on the Subjective Assessment of Medical Probabilities. Medical Decision Making, 2011, 31, 721-729.	2.4	37
82	Title is missing!. Journal of Materials Science Letters, 2002, 21, 293-295.	0.5	36
83	Denaturing HPLC Profiling of the ABCA4 Gene for Reliable Detection of Allelic Variations. Clinical Chemistry, 2004, 50, 1336-1343.	3.2	36
84	Optical properties of Dy3+doped yttrium–aluminium borate. Journal of Physics Condensed Matter, 2004, 16, 465-471.	1.8	36
85	Raman scattering of acoustical modes of silicon nanoparticles embedded in silica matrix. Journal of Raman Spectroscopy, 2006, 37, 161-165.	2.5	36
86	An Overview of Current Microarray-Based Human Globin Gene Mutation Detection Methods. Hemoglobin, 2007, 31, 289-311.	0.8	36
87	Updated clinical overview on cardiac laminopathies: an electrical and mechanical disease. Nucleus, 2018, 9, 380-391.	2.2	36
88	Erbium-activated silica–titania planar waveguides on silica-on-silicon substrates prepared by rf sputtering. Journal of Non-Crystalline Solids, 2001, 284, 230-236.	3.1	35
89	Experimental investigation of photonic band gap influence on enhancement of Raman-scattering in metal-dielectric colloidal crystals. Journal of Applied Physics, 2012, 112, 084303.	2.5	35
90	High-throughput genetic characterization of a cohort of Brugada syndrome patients. Human Molecular Genetics, 2015, 24, 5828-5835.	2.9	35

#	Article	IF	CITATIONS
91	<pre>\$hbox{Er}^{3+}\$ and \$hbox{Ce}^{3+}\$ Codoped Tellurite Optical Fiber for Lasers and Amplifiers in the Near-Infrared Wavelength Region: Fabrication, Optical Characterization, and Prospects. IEEE Photonics Journal, 2012, 4, 194-204.</pre>	2.0	34
92	Optical properties of germanium nanoparticles synthesized by pulsed laser ablation in acetone. Frontiers in Physics, 2014, 2, .	2.1	34
93	From flexible electronics to flexible photonics: A brief overview. Optical Materials, 2021, 115, 111011.	3.6	34
94	Aluminum effect on photoluminescence properties of sol–gel-derived Eu3+-activated silicate glasses. Journal of Non-Crystalline Solids, 2005, 351, 1754-1758.	3.1	33
95	Scanning mutations of the 5′UTR regulatory sequence of l -ferritin by denaturing high-performance liquid chromatography: identification of new mutations. British Journal of Haematology, 2003, 121, 173-179.	2.5	32
96	Erbium-activated silica–zirconia planar waveguides prepared by sol–gel route. Thin Solid Films, 2008, 516, 3094-3097.	1.8	32
97	Controlled Growth of SnO2 Nanocrystals in Eu3+-Doped SiO2â^'SnO2 Planar Waveguides: A Spectroscopic Investigation. Journal of Physical Chemistry C, 2009, 113, 21555-21559.	3.1	32
98	High quality factor Er-doped Fabry–Perot microcavities by sol–gel processing. Journal Physics D: Applied Physics, 2009, 42, 205104.	2.8	32
99	Highly ordered films of quaterthiophene grown by seeded supersonic beams. Applied Physics Letters, 2000, 76, 1845-1847.	3.3	31
100	Spectroscopic and lasing properties of Er3+-doped glass microspheres. Journal of Non-Crystalline Solids, 2006, 352, 2360-2363.	3.1	31
101	3-D rare earth-doped colloidal photonic crystals. Optical Materials, 2009, 31, 1315-1318.	3.6	31
102	Quantum Micro–Nano Devices Fabricated in Diamond by Femtosecond Laser and Ion Irradiation. Advanced Quantum Technologies, 2019, 2, 1900006.	3.9	31
103	Raman and luminescence studies of Tb3+ doped monolithic silica xerogels. Spectrochimica Acta - Part A: Molecular and Biomolecular Spectroscopy, 1998, 54, 2133-2142.	3.9	30
104	EXAFS studies of the local structure of Er3+ ions in silica xerogels co-doped with aluminium. Journal of Non-Crystalline Solids, 2001, 293-295, 112-117.	3.1	30
105	Case report: a subject with a mutation in the ATG start codon of L-ferritin has no haematological or neurological symptoms. Journal of Medical Genetics, 2004, 41, e81-e81.	3.2	30
106	Characterization of a highly photorefractive RF-sputtered SiO2-GeO2 waveguide. Optics Express, 2005, 13, 1696.	3.4	30
107	Metal oxide one dimensional photonic crystals made by RF sputtering and spin coating. Ceramics International, 2015, 41, 8655-8659.	4.8	30
108	Expanding the spectrum of genes responsible for hereditary motor neuropathies. Journal of Neurology, Neurosurgery and Psychiatry, 2019, 90, 1171-1179.	1.9	30

#	Article	IF	CITATIONS
109	Impaired turnover of hyperfused mitochondria in severe axonal neuropathy due to a novel DRP1 mutation. Human Molecular Genetics, 2020, 29, 177-188.	2.9	30
110	Optical spectroscopy of Pr3+ ions in sol–gel derived GeO2–SiO2 planar waveguides. Journal of Non-Crystalline Solids, 1999, 245, 129-134.	3.1	29
111	Intrinsic defects and glass stability in Er 3+ doped TeO 2 glasses and the implications for Er 3+ -doped tellurite fiber amplifiers. Journal of Non-Crystalline Solids, 2003, 326-327, 296-300.	3.1	29
112	Optimization and Characterization of Rare-Earth-Doped Photonic-Crystal-Fiber Amplifier Using Genetic Algorithm. Journal of Lightwave Technology, 2007, 25, 2135-2142.	4.6	29
113	Silver to erbium energy transfer in phosphate glasses. Journal of Non-Crystalline Solids, 2007, 353, 498-501.	3.1	29
114	Origin of Rayleigh scattering and anomaly of elastic properties in vitreous and molten GeO2. Journal of Non-Crystalline Solids, 2008, 354, 3049-3058.	3.1	29
115	Er3+-doped silica–hafnia films for optical waveguides and spherical resonators. Journal of Non-Crystalline Solids, 2009, 355, 1853-1860.	3.1	29
116	Investigation of upconversion luminescence in Yb3+/Tm3+/Ho3+ triply doped antimony-germanate glass and double-clad optical fiber. Optical Materials, 2016, 58, 279-284.	3.6	29
117	Photonic Crystal Stimuli-Responsive Chromatic Sensors: A Short Review. Micromachines, 2020, 11, 290.	2.9	29
118	Er3+-doped tellurite waveguides deposited by excimer laser ablation. Materials Science and Engineering B: Solid-State Materials for Advanced Technology, 2003, 105, 65-69.	3.5	28
119	Reversible photoluminescence quenching in Er3+-doped silica–titania planar waveguides prepared by sol–gel. Journal of Non-Crystalline Solids, 2003, 322, 272-277.	3.1	28
120	Erbium-doped silicate glasses for integrated optical amplifiers and lasers. Journal of Non-Crystalline Solids, 2004, 345-346, 372-376.	3.1	28
121	CO_2 Laser irradiation of GeO_2 planar waveguide fabricated by rf-sputtering. Optical Materials Express, 2013, 3, 1561.	3.0	28
122	Environment segregation of Er3+ emission in bulk sol–gel-derived SiO2–SnO2 glass ceramics. Journal of Materials Science, 2014, 49, 8226-8233.	3.7	28
123	Silver doping of silica-hafnia waveguides containing Tb 3+ /Yb 3+ rare earths for downconversion in PV solar cells. Optical Materials, 2016, 60, 264-269.	3.6	28
124	Gold nanoparticles 1D array as mechanochromic strain sensor. Materials Chemistry and Physics, 2017, 192, 94-99.	4.0	28
125	Rare-earth-doped glasses and ion-exchanged integrated optical amplifiers and lasers. The Philosophical Magazine: Physics of Condensed Matter B, Statistical Mechanics, Electronic, Optical and Magnetic Properties. 2002. 82, 721-734. Local structure around <mml:math <="" td="" xmlns:mml="http://www.w3.org/1998/Math/MathML"><td>0.6</td><td>27</td></mml:math>	0.6	27
126	display="inline"> <mml:msup><mml:mi mathvariant="normal">Er<mml:mrow><mml:mn>3</mml:mn><mml:mo>+</mml:mo></mml:mrow>< xmlns:mml="http://www.w3.org/1998/Math/MathML" display="inline"><mml:mrow><mml:mi mathvariant="normal">Si<mml:msub><mml:mi< td=""><td>:/mml:msi 3.2</td><td>ıp>₂₇mml:mat</td></mml:mi<></mml:msub></mml:mi </mml:mrow></mml:mi </mml:msup>	:/mml:msi 3.2	ıp> ₂₇ mml:mat

#	Article	IF	CITATIONS
127	Spectroscopy and optical characterization of thulium doped TZN glasses. Journal Physics D: Applied Physics, 2010, 43, 135104.	2.8	27
128	Rare earth–activated glass-ceramic in planar format. Optical Engineering, 2011, 50, 071105.	1.0	27
129	Tailoring of the free spectral range and geometrical cavity dispersion of a microsphere by a coating layer. Optics Letters, 2014, 39, 5173.	3.3	27
130	Prospective evaluation of RASSF1A cell-free DNA as a biomarker of pre-eclampsia. Placenta, 2015, 36, 996-1001.	1.5	27
131	Coherent emission from fully Er3+ doped monolithic 1-D dielectric microcavity fabricated by rf-sputtering. Optical Materials, 2019, 87, 107-111.	3.6	27
132	Yellow-to-blue frequency upconversion in Pr3+-doped aluminium fluoride glasses. Journal of Non-Crystalline Solids, 2001, 280, 269-276.	3.1	26
133	Rare-earth-activated fluoride and tellurite glasses: optical and spectroscopic properties. , 2001, , .		26
134	Optical Nanocomposite Planar Waveguides Doped with Rare-Earth and Noble Metal Elements. Journal of Sol-Gel Science and Technology, 2003, 26, 891-896.	2.4	26
135	Design of Er3+ doped SiO2–TiO2 planar waveguide amplifier. Journal of Non-Crystalline Solids, 2003, 322, 278-283.	3.1	26
136	Spectroscopic assessment of silica–titania and silica–hafnia planar waveguides. Philosophical Magazine, 2004, 84, 1659-1666.	1.6	26
137	Investigation of structural and optical properties of sputtered Zirconia thin films. EPJ Applied Physics, 2008, 43, 363-368.	0.7	26
138	COLD-PCR and microarray: two independent highly sensitive approaches allowing the identification of fetal paternally inherited mutations in maternal plasma. Journal of Medical Genetics, 2016, 53, 481-487.	3.2	26
139	Visible to Infrared Diamond Photonics Enabled by Focused Femtosecond Laser Pulses. Micromachines, 2017, 8, 60.	2.9	26
140	Er3+/Yb3+-activated silica–titania planar waveguides for EDPWAs fabricated by rf-sputtering. Journal of Non-Crystalline Solids, 2003, 322, 289-294.	3.1	25
141	Rare-earth doped photonic crystal microcavities prepared by sol–gel. Journal of Non-Crystalline Solids, 2007, 353, 490-493.	3.1	25
142	Synthesis, structure and spectroscopic properties of luminescent GdVO4:Dy3+ and DyVO4 particles. Optical Materials, 2018, 76, 308-316.	3.6	25
143	The role of clinical and neuroimaging features in the diagnosis of CADASIL. Journal of Neurology, 2018, 265, 2934-2943.	3.6	25
144	Crystallization of silica xerogels: A study by raman and fluorescence spectroscopy. Journal of Sol-Gel Science and Technology, 1997, 8, 391-395.	2.4	24

#	Article	IF	CITATIONS
145	Fluorescence line narrowing study of Cr ions in cordierite glass nucleating MgAlO nanocrystals. Optical Materials, 2000, 13, 373-379.	3.6	24
146	Femtosecond laser direct writing of gratings and waveguides in high quantum efficiency erbium-doped Baccarat glass. Journal Physics D: Applied Physics, 2009, 42, 205106.	2.8	24
147	Controlled SnO ₂ nanocrystal growth in SiO ₂ –SnO ₂ glassâ€ceramic monoliths. Journal of Raman Spectroscopy, 2012, 43, 869-875.	2.5	24
148	Structural and spectroscopic properties of Eu3+-activated nanocrystalline tetraphosphates loaded in silica–hafnia thin film. Journal of Non-Crystalline Solids, 2014, 401, 32-35.	3.1	24
149	Photoluminescence and lasing in whispering gallery mode glass microspherical resonators. Journal of Luminescence, 2016, 170, 755-760.	3.1	24
150	Waveguide Raman spectroscopy: a non-destructive tool for the characterization of amorphous thin films. Journal of Molecular Structure, 1999, 480-481, 169-178.	3.6	23
151	Erbium-activated aluminum fluoride glasses: optical and spectroscopic properties. Journal of Non-Crystalline Solids, 2001, 284, 243-248.	3.1	23
152	Erbium-doped GeO2–TiO2 sol–gel waveguides. Journal of Non-Crystalline Solids, 2003, 322, 295-299.	3.1	23
153	Analysis of ferritin genes in Parkinson disease. Clinical Chemistry and Laboratory Medicine, 2007, 45, 1450-6.	2.3	23
154	Preparation and characterization of ZnO particles embedded in organic–inorganic planar waveguide by sol–gel route. Journal of Non-Crystalline Solids, 2009, 355, 1132-1135.	3.1	23
155	X-ray photoelectron spectroscopy of Er3+-activated SiO2–HfO2glass-ceramic waveguides. Journal Physics D: Applied Physics, 2009, 42, 015408.	2.8	23
156	Titanate Nanosheets as High Refractive Layer in Vertical Microcavity Incorporating Semiconductor Quantum Dots. Journal of Physical Chemistry C, 2010, 114, 18423-18428.	3.1	23
157	Laser surface structuring of diamond with ultrashort Bessel beams. Scientific Reports, 2018, 8, 14021.	3.3	23
158	Upconversion Luminescence of Silica–Calcia Nanoparticles Co-doped with Tm3+ and Yb3+ Ions. Materials, 2021, 14, 937.	2.9	23
159	Identification of two novel mutations in the 5'-untranslated region of H-ferritin using denaturing high performance liquid chromatography scanning. Haematologica, 2003, 88, 1110-6.	3.5	23
160	Er3+/Yb3+ Co-Activated Silica-Alumina Monolithic Xerogels. Journal of Sol-Gel Science and Technology, 2003, 26, 943-946.	2.4	22
161	Short-range order around Er3+ in silica waveguides containing aluminium, titanium and hafnium. Optical Materials, 2006, 28, 864-867.	3.6	22
162	Mechanism of low-frequency Raman scattering from the acoustic vibrations of dielectric nanoparticles. Physical Review B, 2006, 74, .	3.2	22

#	Article	IF	CITATIONS
163	XPS and UPS investigation of the diamond surface oxidation by UV irradiation. Diamond and Related Materials, 2009, 18, 804-807.	3.9	22
164	Modeling of Whispering Gallery Modes for Rare Earth Spectroscopic Characterization. IEEE Photonics Technology Letters, 2015, 27, 1861-1863.	2.5	22
165	Hybrid 1-D dielectric microcavity: Fabrication and spectroscopic assessment of glass-based sub-wavelength structures. Ceramics International, 2015, 41, 7429-7433.	4.8	22
166	SiO2-SnO2:Er3+ Glass-Ceramic Monoliths. Applied Sciences (Switzerland), 2018, 8, 1335.	2.5	22
167	Impaired testicular signaling of vitamin A and vitamin K contributes to the aberrant composition of the extracellular matrix in idiopathic germ cell aplasia. Fertility and Sterility, 2019, 111, 687-698.	1.0	22
168	Optical properties and structural characterization of erbium-activated SiO ₂ -TiO ₂ planar waveguides prepared by rf sputtering. The Philosophical Magazine: Physics of Condensed Matter B, Statistical Mechanics, Electronic, Optical and Magnetic Properties, 1999, 79, 2103-2112.	0.6	21
169	The role of oxygen in the one step amination process of nanocrystalline diamond surface. Diamond and Related Materials, 2011, 20, 990-994.	3.9	21
170	Downconversion in Pr3+–Yb3+ co-doped ZBLA fluoride glasses. Journal of Luminescence, 2015, 161, 198-201.	3.1	21
171	Pulsed Bessel beam-induced microchannels on a diamond surface for versatile microfluidic and sensing applications. Optical Materials Express, 2017, 7, 1962.	3.0	21
172	Polarized micro-Raman studies of femtosecond laser written stress-induced optical waveguides in diamond. Applied Physics Letters, 2018, 112, .	3.3	21
173	Homogeneous line width in a zinc borate glass activated by Eu3+. Journal of Non-Crystalline Solids, 1997, 220, 217-221.	3.1	20
174	Effect of Pr3+ Doping on the OH Content of Silica Xerogels. Journal of Sol-Gel Science and Technology, 1998, 13, 599-603.	2.4	20
175	The structure of Er 3+ -doped oxy-fluoride transparent glass-ceramics studied by Raman scattering. Europhysics Letters, 2003, 64, 529-535.	2.0	20
176	Erbium-doped thin amorphous carbon films prepared by mixed CVD sputtering. Applied Surface Science, 2004, 238, 117-120.	6.1	20
177	Nanocomposite Er–Ag silicate glasses. Journal of Optics, 2006, 8, S450-S454.	1.5	20
178	Characterization of thiol-functionalized carbon nanotubes on gold surfaces. Surface Science, 2010, 604, 1414-1419.	1.9	20
179	Application of molecular dynamics techniques and luminescent probes to the study of glass structure: the SiO2–GeO2 case. Journal of Non-Crystalline Solids, 2001, 284, 68-72.	3.1	19
180	Chalcogenide glass thin film waveguides deposited by excimer laser ablation. Applied Surface Science, 2003, 208-209, 632-637.	6.1	19

#	Article	IF	CITATIONS
181	Integrated optical amplifiers and microspherical lasers based on erbium-doped oxide glasses. Optical Materials, 2005, 27, 1711-1717.	3.6	19
182	Structure and properties of Ti4+-ureasil organic-inorganic hybrids. Journal of the Brazilian Chemical Society, 2006, 17, 443-452.	0.6	19
183	Erbium-activated modified silica glasses with high 4113/2 luminescence quantum yield. Optical Materials, 2006, 28, 1325-1328.	3.6	19
184	Er3+activated silica-hafnia glass-ceramics planar waveguides. , 2006, 6183, 438.		19
185	About the role of phase matching between a coated microsphere and a tapered fiber: experimental study. Optics Express, 2013, 21, 20954.	3.4	19
186	Comparison between glass and glass-ceramic silica-hafnia matrices on the down-conversion efficiency of Tb3+/Yb3+ rare earth ions. Optical Materials, 2019, 87, 102-106.	3.6	19
187	Erbium-Doped Tin-Silicate Sol–Gel-Derived Glass-Ceramic Thin Films: Effect of Environment Segregation on the Er ³⁺ Emission. Science of Advanced Materials, 2015, 7, 301-308.	0.7	19
188	Decomposition and first stages of the crystallization in fluorozirconate glasses. Journal of Non-Crystalline Solids, 1988, 99, 210-221.	3.1	18
189	Molecular dynamics study of Eu ³⁺ in an aqueous solution: Luminescence spectrum from simulated environments. The Philosophical Magazine: Physics of Condensed Matter B, Statistical Mechanics, Electronic, Optical and Magnetic Properties, 1998, 77, 681-688.	0.6	18
190	On a qualitative model for the incorporation of fluoride nano-crystals within an oxide glass network in oxy-fluoride glass-ceramics. Journal of Non-Crystalline Solids, 2004, 337, 191-195.	3.1	18
191	UV photoimprinting of channel waveguides on active SiO2–GeO2 sputtered thin films. Applied Physics Letters, 2006, 89, 121102.	3.3	18
192	CO2 laser annealing on erbium-activated glass–ceramic waveguides for photonics. Optical Materials, 2009, 31, 1310-1314.	3.6	18
193	Er3+/Yb3+-activated silica-hafnia planar waveguides for photonics fabricated by rf-sputtering. Journal of Non-Crystalline Solids, 2009, 355, 1176-1179.	3.1	18
194	Luminescent short thiol-functionalized multi-wall carbon nanotubes. Diamond and Related Materials, 2011, 20, 1046-1049.	3.9	18
195	Light-opals interaction modeling by direct numerical solution of Maxwell's equations. Optics Express, 2014, 22, 27739.	3.4	18
196	Sol–Gel-Derived Glass-Ceramic Photorefractive Films for Photonic Structures. Crystals, 2017, 7, 61.	2.2	18
197	New molecular approaches to Alzheimer's disease. Clinical Biochemistry, 2019, 72, 81-86.	1.9	18
198	Evaluation of three advanced methodologies, COLD-PCR, microarray and ddPCR, for identifying the mutational status by liquid biopsies in metastatic colorectal cancer patients. Clinica Chimica Acta, 2019, 489, 136-143.	1.1	18

#	Article	IF	CITATIONS
199	On the optical absorption and nonlinearity of silica films containing metal nanoparticles. The Philosophical Magazine: Physics of Condensed Matter B, Statistical Mechanics, Electronic, Optical and Magnetic Properties, 2002, 82, 735-744.	0.6	18
200	Relative role of <i>APC</i> and <i>MUTYH</i> mutations in the pathogenesis of familial adenomatous polyposis. Scandinavian Journal of Gastroenterology, 2009, 44, 1092-1100.	1.5	17
201	Photoluminescence in Er3+/Yb3+-doped silica-titania inverse opal structures. Journal of Sol-Gel Science and Technology, 2010, 55, 52-58.	2.4	17
202	Influence of Nd3+ doping on the structural and near-IR photoluminescence properties of nanostructured TiO2 films. Energy Procedia, 2011, 10, 167-171.	1.8	17
203	White light emission through energy transfer processes in barium gallo-germanate glasses co-doped with Dy3+-Ln3+ (Ln =Ce, Tm). Optical Materials, 2019, 87, 63-69.	3.6	17
204	Rare earth elements and urban mines: Critical strategies for sustainable development. Ceramics International, 2020, 46, 26247-26250.	4.8	17
205	Assessment of SnO2-nanocrystal-based luminescent glass-ceramic waveguides for integrated photonics. Ceramics International, 2021, 47, 5534-5541.	4.8	17
206	Photosensitive erbium doped tin-silicate glass. Journal of Non-Crystalline Solids, 2002, 311, 217-222.	3.1	16
207	Optical studies of two dimensional gratings in fused silica, GE 124, and Foturanâ,,¢ glasses fabricated using femtosecond laser pulses. Optics Communications, 2009, 282, 4537-4542.	2.1	16
208	Solvent sensitive polymer composite structures. Optical Materials, 2013, 36, 130-134.	3.6	16
209	Whispering gallery mode profiles in a coated microsphere. European Physical Journal: Special Topics, 2014, 223, 1959-1969.	2.6	16
210	New trend in non-invasive prenatal diagnosis. Clinica Chimica Acta, 2015, 451, 9-13.	1.1	16
211	Communicating Down syndrome risk according to maternal age: "1-in- <i>X</i> ―effect on perceived risk. Prenatal Diagnosis, 2015, 35, 777-782.	2.3	16
212	Structural and luminescence study of Ce3+ and Tb3+ doped Ca3Sc2Si3O12 garnets obtained by freeze-drying synthesis method. Optical Materials, 2015, 46, 109-114.	3.6	16
213	Sol-gel synthesis and characterization of undoped and Al-doped ZnO thin films for memristive application. AIP Advances, 2016, 6, .	1.3	16
214	DNA microarray-based solid-phase PCR on copoly (DMA–NAS–MAPS) silicon coated slides: An example of relevant clinical application. Biosensors and Bioelectronics, 2016, 78, 367-373.	10.1	16
215	Synthesis and Post-Annealing of Cu2ZnSnS4 Absorber Layers Based on Oleylamine/1-dodecanethiol. Materials, 2019, 12, 3320.	2.9	16
216	Influence of the rare earth ions concentration on luminescence properties of barium gallo-germanate glasses for white lighting. Journal of Luminescence, 2019, 211, 375-381.	3.1	16

#	Article	IF	CITATIONS
217	Fabrication, modelling and assessment of hybrid 1-D elastic Fabry Perot microcavity for mechanical sensing applications. Ceramics International, 2019, 45, 7785-7788.	4.8	16
218	First stages of the crystallization in fluorozirconate glasses. Journal of Non-Crystalline Solids, 1989, 111, 238-244.	3.1	15
219	Waveguide luminescence and Raman spectroscopy: Characterization of an inhomogeneous film at different depths. Applied Physics Letters, 1999, 75, 1529-1531.	3.3	15
220	Photoluminescence of Erbium-Doped Silicate Sol-Gel Planar Waveguides. Journal of Sol-Gel Science and Technology, 2004, 31, 317-322.	2.4	15
221	Enhanced spectroscopic properties at 1.5 μ4m in Er3+/Yb3+-activated silica–titania planar waveguides fabricated by rf-sputtering. Optical Materials, 2004, 25, 117-122.	3.6	15
222	Relationship between structure and optical properties in rare earth-doped hafnium and silicon oxides: Modeling and spectroscopic measurements. Journal of Non-Crystalline Solids, 2008, 354, 4719-4722.	3.1	15
223	Extended transfer matrix modeling of an erbium-doped cavity with SiO2/TiO2 Bragg reflectors. Optical Materials, 2009, 31, 1306-1309.	3.6	15
224	Synthesis and characterization of PMMA-based superhydrophobic surfaces. Colloid and Polymer Science, 2012, 290, 315-322.	2.1	15
225	High quality-factor optical resonators. Physica Scripta, 2014, T162, 014032.	2.5	15
226	Morphologic, structural, and optical characterization of sol-gel derived TiO2 thin films for memristive devices. Physica Status Solidi C: Current Topics in Solid State Physics, 2015, 12, 192-196.	0.8	15
227	Sol–gel-derived photonic structures handling erbium ions luminescence. Optical and Quantum Electronics, 2015, 47, 117-124.	3.3	15
228	Width of the excitonic absorption peak and size of CdSxSe1â^'x semiconductor nanocrystallites. Journal of Non-Crystalline Solids, 1992, 151, 95-101.	3.1	14
229	X-ray diffraction and Raman scattering measurements on silica xerogels. Journal of Non-Crystalline Solids, 2002, 307-310, 135-141.	3.1	14
230	X-Ray Absorption and Diffraction Studies of Pr3+, Tb3+ and Er3+-Activated Silica Gels. Journal of Sol-Gel Science and Technology, 2003, 26, 267-271.	2.4	14
231	Genotyping Î ² -Globin Gene Mutations on Copolymer-Coated Glass Slides with the Ligation Detection Reaction. Clinical Chemistry, 2008, 54, 1657-1663.	3.2	14
232	Characterization of Er3+-doped fluoride glass ceramics waveguides containing LaF3 nanocrystals. Journal of Luminescence, 2009, 129, 1637-1640.	3.1	14
233	Design of Rare-Earth-Doped Microspheres. IEEE Photonics Technology Letters, 2010, 22, 422-424.	2.5	14
234	Structural-microstructural characterization and optical properties of Eu3+,Tb3+-codoped LaPO4·nH2O and LaPO4 nanorods hydrothermally synthesized with microwaves. Ceramics International, 2018, 44, 11993-12001.	4.8	14

#	Article	IF	CITATIONS
235	Blue to NIR down-conversion in Tm3+/Yb3+-codoped fluorozirconate glasses compared to Pr3+/Yb3+ ion-pair. Journal of Luminescence, 2018, 193, 22-28.	3.1	14
236	2D Optical Gratings Based on Hexagonal Voids on Transparent Elastomeric Substrate. Micromachines, 2018, 9, 345.	2.9	14
237	Ag nanoaggregates as efficient broadband sensitizers for Tb3+ ions in silica-zirconia ion-exchanged sol-gel glasses and glass-ceramics. Optical Materials, 2018, 84, 668-674.	3.6	14
238	Fluoroindate Glass Co-Doped with Yb3+/Ho3+ as a 2.85 μm Luminescent Source for MID-IR Sensing. Sensors, 2021, 21, 2155.	3.8	14
239	Title is missing!. European Physical Journal B, 2002, 25, 11-17.	1.5	14
240	Brillouin scattering in planar waveguides. Physical Review B, 1998, 58, R547-R550.	3.2	13
241	X-ray photoelectron spectroscopy of erbium-activated-silica–hafnia waveguides. Journal of Non-Crystalline Solids, 2007, 353, 502-505.	3.1	13
242	Enhanced spectroscopic properties in Er3+/Yb3+-activated fluoride glass–ceramics planar waveguides. Optical Materials, 2009, 31, 1288-1291.	3.6	13
243	Photoluminescence spectra of an optically pumped erbium-doped micro-cavity with SiO2/TiO2 distributed Bragg reflectors. Journal of Luminescence, 2009, 129, 1989-1993.	3.1	13
244	Pr3+–Yb3+ odoped lanthanum fluorozirconate glasses and waveguides for visible laser emission. Journal of Non-Crystalline Solids, 2012, 358, 2695-2700.	3.1	13
245	Fabrication and optical properties of assembled gold nanoparticles film on elastomeric substrate. Colloids and Surfaces A: Physicochemical and Engineering Aspects, 2015, 482, 431-437.	4.7	13
246	Towards low voltage resistive switch in sol-gel derived TiO2/Ta2O5 stack thin films. Materials and Design, 2016, 105, 359-365.	7.0	13
247	Crystallization and optical properties of Tm ³⁺ /Yb ³⁺ -co-doped KLaF ₄ glass-ceramics. CrystEngComm, 2017, 19, 967-974.	2.6	13
248	Rare-earth activated SnO2 photoluminescent thin films on flexible glass: Synthesis, deposition and characterization. Optical Materials, 2022, 124, 111978.	3.6	13
249	Fluorescence line narrowing inCr3+-doped gallium gadolinium garnet under a magnetic field. Physical Review B, 1991, 43, 3646-3648.	3.2	12
250	Optical spectroscopy of Eu ³⁺ -doped silica gels. The Philosophical Magazine: Physics of Condensed Matter B, Statistical Mechanics, Electronic, Optical and Magnetic Properties, 1995, 71, 633-640.	0.6	12
251	Waveguide Raman Spectroscopy as a Tool for the Detection of Nanometric Metallic Particles in Glasses. Journal of Raman Spectroscopy, 1996, 27, 793-797.	2.5	12
252	Erbium-activated monolithic silica xerogels and silica-titania planar waveguides: optical and spectroscopic characterization. , 2001, , .		12

#	Article	IF	CITATIONS
253	Intrinsic Defect Related Photoluminescence in TeO2-Based Glasses. Physica Status Solidi A, 2001, 187, R4-R6.	1.7	12
254	Laser irradiation, ion implantation, and e-beam writing of integrated optical structures. , 2005, , .		12
255	UV assisted local crystallization in Er3+ doped oxy-fluoride glass. Journal of Non-Crystalline Solids, 2007, 353, 506-509.	3.1	12
256	SiO 2 -P 2 O 5 -HfO 2 -Al 2 O 3 -Na 2 O glasses activated by Er 3+ ions: From bulk sample to planar waveguide fabricated by rf-sputtering. Optical Materials, 2017, 63, 153-157.	3.6	12
257	Fluorescent Aptamer Immobilization on Inverse Colloidal Crystals. Sensors, 2018, 18, 4326.	3.8	12
258	Colloidal crystals based portable chromatic sensor for butanol isomers and water mixtures detection. Optical Materials, 2019, 90, 152-158.	3.6	12
259	Title is missing!. Journal of Sol-Gel Science and Technology, 2000, 19, 569-572.	2.4	11
260	Metal nanocluster formation in silica films prepared by rf-sputtering: an experimental study. European Physical Journal B, 2002, 25, 11-17.	1.5	11
261	Novel Er-doped SiC/SiO2 nanocomposites: Synthesis via polymer pyrolysis and their optical characterization. Journal of the European Ceramic Society, 2005, 25, 277-281.	5.7	11
262	Patterning of Sol–Gel Hybrid Organic–Inorganic Film Doped with Luminescent Semiconductor Quantum Dots. Journal of Nanoscience and Nanotechnology, 2009, 9, 1858-1864.	0.9	11
263	Luminescence and structural analysis of Ce ³⁺ and Er ³⁺ doped and Ce ³⁺ –Er ³⁺ codoped Ca ₃ Sc ₂ Si ₃ O ₁₂ garnets: influence of the doping concentration in the energy transfer processes. RSC Advances. 2016. 6. 15054-15061.	3.6	11
264	Genotype/Phenotype Relationship in a Consanguineal Family With Brugada Syndrome Harboring the R1632C Missense Variant in the SCN5A Gene. Frontiers in Physiology, 2019, 10, 666.	2.8	11
265	A novel homozygous mutation in the TRDN gene causes a severe form of pediatric malignant ventricular arrhythmia. Heart Rhythm, 2020, 17, 296-304.	0.7	11
266	Generation of β Cells from iPSC of a MODY8 Patient with a Novel Mutation in the Carboxyl Ester Lipase (<i>CEL</i>) Gene. Journal of Clinical Endocrinology and Metabolism, 2021, 106, e2322-e2333.	3.6	11
267	Nonlinear effects in microcrystalline semiconductors. Journal of Luminescence, 1991, 48-49, 306-308.	3.1	10
268	Molecular dynamics simulation of Eu3+ in aqueous solution comparison with experimental luminescence spectra. Journal of Luminescence, 1997, 72-74, 567-569.	3.1	10
269	Structural properties of erbium-activated silica-titania glasses: modeling by molecular dynamics method. , 2000, 3942, 243.		10
270	Rare-earth-doped glasses and ion-exchanged integrated optical amplifiers and lasers. The Philosophical Magazine: Physics of Condensed Matter B, Statistical Mechanics, Electronic, Optical and Magnetic Properties, 2002, 82, 721-734.	0.6	10

#	Article	IF	CITATIONS
271	Integrated optical amplifiers based on rare-earth doped oxide glasses. , 2003, 5061, 34.		10
272	Frequency converter layers based on terbium and ytterbium activated HfO 2 glass-ceramics. Proceedings of SPIE, 2010, , .	0.8	10
273	Novel multifunctional nanocomposites from titanate nanosheets and semiconductor quantum dots. Optical Materials, 2011, 33, 1839-1846.	3.6	10
274	Local Site Distribution of Oxygen in Silicon-Rich Oxide Thin Films: A Tool to Investigate Phase Separation. Journal of Physical Chemistry C, 2012, 116, 10039-10047.	3.1	10
275	Time-resolved photoluminescence studies in Eu-doped SiO 2 – HfO 2 – ZnO glass-ceramic waveguides. Ceramics International, 2017, 43, 1145-1149.	4.8	10
276	Determination of reverse cross-relaxation process constant in Tm-doped glass by ^3H_4 fluorescence decay tail fitting. Optical Materials Express, 2017, 7, 3760.	3.0	10
277	Photonic band edge assisted spontaneous emission enhancement from all Er3+ 1-D photonic band gap structure. Optical Materials, 2018, 80, 106-109.	3.6	10
278	Ag-Sensitized Yb3+ Emission in Glass-Ceramics. Micromachines, 2018, 9, 380.	2.9	10
279	X-ray photoemission study of Pr ³⁺ in zinc borate glasses. The Philosophical Magazine: Physics of Condensed Matter B, Statistical Mechanics, Electronic, Optical and Magnetic Properties, 1999, 79, 2145-2155.	0.6	9
280	Erbium-activated silica-titania planar waveguides prepared by rf-sputtering. , 2001, , .		9
281	Molecular diagnostics by microelectronic microchips. Expert Review of Molecular Diagnostics, 2005, 5, 183-192.	3.1	9
282	Er3+-activated sol–gel silica confined structures for photonic applications. Optical Materials, 2009, 31, 1275-1279.	3.6	9
283	Er ³⁺ /Yb ³⁺ /Ce ³⁺ Co-Doped Fluoride Glass Ceramics Waveguides for Application in the 1.5Âμm Telecommunication Window. Advances in Science and Technology, 2010, 71, 16-21.	0.2	9
284	Highly photorefractive Eu ³⁺ activated sol-gel SiO 2 -SnO 2 thin film waveguides. Proceedings of SPIE, 2010, , .	0.8	9
285	Sequence Variations in Mitochondrial Ferritin: Distribution in Healthy Controls and Different Types of Patients. Genetic Testing and Molecular Biomarkers, 2010, 14, 793-796.	0.7	9
286	XPS and UPS in situ study of oxygen thermal desorption from nanocrystalline diamond surface oxidized by different process. Diamond and Related Materials, 2011, 20, 560-563.	3.9	9
287	Up-conversion visible emission in rare-earth doped fluoride glass waveguides. Optical Engineering, 2014, 53, 071814.	1.0	9
288	Thermo optical coefficient of tin-oxide films measured by ellipsometry. Journal of Applied Physics, 2015, 118, .	2.5	9

#	Article	IF	CITATIONS
289	Up-conversion luminescence of RE3+ -doped polymer composites KGd(WO4)2&PMMA. Optical Materials, 2019, 88, 366-371.	3.6	9
290	Low frequency light scattering in silica xerogels. Journal of Physics Condensed Matter, 1999, 11, A207-A211.	1.8	8
291	Pressure effect on the structure and the luminescence of rare-earth ions doped glasses: an investigation by molecular dynamics simulation. Journal of Luminescence, 2000, 87-89, 691-693.	3.1	8
292	Erbium Photoluminescence in Hydrogenated Amorphous Carbon. Physica Status Solidi (B): Basic Research, 2002, 234, R1-R3.	1.5	8
293	Sol-gel erbium-doped silica-hafnia planar and channel waveguides. , 2003, , .		8
294	Single-Nucleotide Polymorphism and Mutation Identification by the Nanogen Microelectronic Chip Technology. , 2005, 114, 93-106.		8
295	Influence of PrCl3/PrF3 on the optical and spectroscopic properties of fluorogallate and fluoro-gallo-indate glasses. Optical Materials, 2006, 28, 441-447.	3.6	8
296	Pulsed Laser Deposition of Er doped tellurite films on large area. Journal of Physics: Conference Series, 2007, 59, 475-478.	0.4	8
297	Rare Earth-Activated Silica-Based Nanocomposites. Journal of Nanomaterials, 2007, 2007, 1-6.	2.7	8
298	Highâ€ŧhroughput mutational screening for betaâ€ŧhalassemia by singleâ€nucleotide extension. Electrophoresis, 2007, 28, 4289-4294.	2.4	8
299	Development of new substrates for highâ€sensitive genotyping of minority mutated alleles. Electrophoresis, 2008, 29, 4714-4722.	2.4	8
300	Design and fabrication of mechanochromic photonic crystals as strain sensor. Proceedings of SPIE, 2015, , .	0.8	8
301	Highly integrated lab-on-a-chip for fluorescence detection. Optical Engineering, 2016, 55, 097102.	1.0	8
302	Quasi-hemispherical voids micropatterned PDMS as strain sensor. Optical Materials, 2018, 86, 408-413.	3.6	8
303	Spatial energy transfer: Cr3+clustering around vacancies in MgO crystal. Journal of Physics C: Solid State Physics, 1986, 19, 3253-3262.	1.5	7
304	A study of Raman spectroscopy and low-temperature specific heat in gel-synthesized amorphous silica. Journal of Non-Crystalline Solids, 2001, 280, 249-254.	3.1	7
305	<title>Microsphere laser in Er<formula><sup><roman>3+</roman></sup></formula>-doped oxide
glasses</title> .,2004,,.		7
306	Rare-earth-doped silica-based glasses for photonic applications. Journal of Non-Crystalline Solids, 2007, 353, 753-756.	3.1	7

#	Article	IF	CITATIONS
307	Effect of Eu3+ and Ce3+codoping on the relaxation of Er3+ in silica-hafnia and tellurite glasses. Physica Status Solidi C: Current Topics in Solid State Physics, 2007, 4, 793-796.	0.8	7
308	Coupling light to whispering gallery mode resonators. Proceedings of SPIE, 2014, , .	0.8	7
309	Evaluation of damaging effects of splicing mutations: Validation of an in vitro method for diagnostic laboratories. Clinica Chimica Acta, 2014, 436, 276-282.	1.1	7
310	Numerical modeling of the impact of pump wavelength on Yb-doped fiber amplifier performance. Optical and Quantum Electronics, 2016, 48, 1.	3.3	7
311	Nanocrystalline lanthanide tetraphosphates: Energy transfer processes in samples co-doped with Pr 3+ /Yb 3+ and Tm 3+ /Yb 3+. Optical Materials, 2017, 74, 159-165.	3.6	7
312	Yb3+ concentration influences UV–Vis to NIR energy conversion in nanostructured Pr3+ and Yb3+ co-doped SiO2-Nb2O5 materials for photonics. Journal of Luminescence, 2018, 199, 454-460.	3.1	7
313	About the Implementation of Frequency Conversion Processes in Solar Cell Device Simulations. Micromachines, 2018, 9, 435.	2.9	7
314	Novel SCN5A p.W697X Nonsense Mutation Segregation in a Family with Brugada Syndrome. International Journal of Molecular Sciences, 2019, 20, 4920.	4.1	7
315	Design, fabrication and assessment of an optomechanical sensor for pressure and vibration detection using flexible glass multilayers. Optical Materials, 2021, 115, 111023.	3.6	7
316	Eu3+ as a Powerful Structural and Spectroscopic Tool for Glass Photonics. Materials, 2022, 15, 1847.	2.9	7
317	Dynamical processes in sol-gel derived rare-earth doped glasses. Journal of Sol-Gel Science and Technology, 1994, 2, 771-774.	2.4	6
318	Luminescence of Pr 3+ ions in sodium β-Al 2 O 3 crystals. Journal of Luminescence, 1994, 60-61, 216-219.	3.1	6
319	NMR and luminescence studies on the formation of ternary adducts between HSA and Ln(III)–malonate complexes (Ln=Eu, Gd, Tb). BBA - Proteins and Proteomics, 1998, 1385, 7-16.	2.1	6
320	Line width measurements of Cr3+ in a zinc borate glass. Journal of Non-Crystalline Solids, 1998, 240, 232-236.	3.1	6
321	Fabrication and characterization of optical planar waveguides activated by erbium ions for 1.5-μm applications. , 2004, 5451, 574.		6
322	Spectroscopic assessment of rare-earth activated planar waveguides and microcavities. Applied Surface Science, 2005, 248, 3-7.	6.1	6
323	Diagnostic techniques for photonic materials based on Raman and Brillouin spectroscopies. Optoelectronics Letters, 2007, 3, 188-191.	0.8	6
324	Raman scattering on quadrupolar vibrational modes of spherical nanoparticles. Journal of Applied Physics, 2008, 104, .	2.5	6

#	Article	IF	CITATIONS
325	Photonic properties and applications of glass micro―and nanospheres. Physica Status Solidi (A) Applications and Materials Science, 2009, 206, 898-903.	1.8	6
326	Glass-Ceramic waveguides: Fabrication and properties. , 2010, , .		6
327	Fabrication and characterization of colloidal crystals infiltrated with metallic nanoparticles. Proceedings of SPIE, 2010, , .	0.8	6
328	Erbium doped silicaâ€hafnia glass ceramic waveguides. Physica Status Solidi C: Current Topics in Solid State Physics, 2011, 8, 2875-2879.	0.8	6
329	Surface characterization of thin silicon-rich oxide films. Journal of Molecular Structure, 2011, 993, 214-218.	3.6	6
330	Sol-Gel-Derived Erbium-Activated Silica-Titania and Silica-Hafnia Planar Waveguides for 1.5µm Application in C Band of Telecommunication. Spectroscopy Letters, 2014, 47, 381-386.	1.0	6
331	CO ₂ Laser irradiation of GeO ₂ planar waveguide fabricated by rf-sputtering. IOP Conference Series: Materials Science and Engineering, 2015, 73, 012006.	0.6	6
332	Raman spectroscopy of femtosecond laser written low propagation loss optical waveguides in Schott N-SF8 glass. Optical Materials, 2017, 72, 626-631.	3.6	6
333	Current scenario of the genetic testing for rare neurological disorders exploiting next generation sequencing. Neural Regeneration Research, 2021, 16, 475.	3.0	6
334	Manufacturing Optically Transparent Thick Zirconia Ceramics by Spark Plasma Sintering with the Use of Collector Pressing. Applied Sciences (Switzerland), 2021, 11, 1304.	2.5	6
335	Luminescent Ink Based on Upconversion of NaYF4:Er,Yb@MA Nanoparticles: Environmental Friendly Synthesis and Structural and Spectroscopic Assessment. Molecules, 2021, 26, 1041.	3.8	6
336	Magnetic-field study of the energy levels and nonradiative transitions in MgO:Cr3+. Physical Review B, 1982, 25, 3063-3072.	3.2	5
337	Site selection spectroscopy of SiO2:Eu3+ gels. Journal of Sol-Gel Science and Technology, 1994, 2, 783-786.	2.4	5
338	<title>Er<formula><sup><roman>3+ </roman></sup></formula>and
Er<formula><sup><roman>3+</roman></sup></formula>/Yb<formula><sup><roman>3+
</roman></sup></formula>co-doped silicate glass waveguides</title> . , 1999, 3749, 755.		5
339	Low-frequency light scattering in silica xerogels: Influence of the heat treatment. The Philosophical Magazine: Physics of Condensed Matter B, Statistical Mechanics, Electronic, Optical and Magnetic Properties, 1999, 79, 2081-2089.	0.6	5
340	Low-wavenumber Raman scattering spectroscopy in studies of new gallium-doped silica glass-based transparent vitroceramic medium. Journal of Raman Spectroscopy, 2001, 32, 643-647.	2.5	5
341	Brillouin scattering in planar waveguides. I. Numerical model. Journal of Applied Physics, 2003, 94, 4876.	2.5	5
342	Er3+/Yb3+-codoped silica–germania sputtered films: structural and spectroscopic characterization. Journal of Non-Crystalline Solids, 2006, 352, 2585-2588.	3.1	5

#	Article	IF	CITATIONS
343	Fabrication and optical assessment of sol-gel-derived photonic bandgap dielectric structures. , 2006, 6182, 454.		5
344	Er3+-activated silica inverse opals synthesized by the solgel method. Optoelectronics Letters, 2007, 3, 184-187.	0.8	5
345	Photonic properties of erbium activated coated microspheres. , 2008, , .		5
346	Structural investigation of photonic materials at the nanolevel using XPS. Journal of Non-Crystalline Solids, 2009, 355, 1157-1159.	3.1	5
347	Spatially localized UV-induced crystallization of SnO 2 in photorefractive SiO 2 -SnO 2 thin film. Proceedings of SPIE, 2010, , .	0.8	5
348	Influence of phosphorous precursors on spectroscopic properties of Er3+-activated SiO2-HfO2-P2O5planar waveguides. Journal of Physics: Conference Series, 2014, 566, 012018.	0.4	5
349	Rare-earth doped materials for optical waveguides. , 2015, , .		5
350	Glass-based 1-D dielectric microcavities. Optical Materials, 2016, 61, 11-14.	3.6	5
351	Challenges and future trends in fiber lasers. , 2016, , .		5
352	Fractional-Order Theory of Thermoelasticicty. I: Generalization of the Fourier Equation. Journal of Engineering Mechanics - ASCE, 2018, 144, 04017164.	2.9	5
353	Rare-earth doped glasses and light managing in solar cells. Journal of Physics: Conference Series, 2019, 1221, 012028.	0.4	5
354	Class ceramics for frequency conversion. , 2020, , 391-414.		5
355	MSH6 gene pathogenic variant identified in familial pancreatic cancer in the absence of colon cancer. European Journal of Gastroenterology and Hepatology, 2020, 32, 345-349.	1.6	5
356	Opal-Based Photonic Crystal Heterostructures. Optics and Photonics Journal, 2012, 02, 206-210.	0.4	5
357	Sol-gel-derived transparent glass-ceramics for photonics. Optical Materials, 2022, 130, 112577.	3.6	5
358	Structure-property behavior during aging of sol-gel-derived silica modified with Si–H and Si–CH3 groups. Journal of Materials Research, 1999, 14, 2100-2106.	2.6	4
359	Brillouin scattering in planar waveguides. II. Experiments. Journal of Applied Physics, 2003, 94, 4882.	2.5	4
360	Tm3+-Activated Transparent Oxyfluoride Glass Ceramics: A Study by Raman Scattering of the Nanocrystal Size Distribution. Glass Physics and Chemistry, 2005, 31, 519-524.	0.7	4

#	Article	IF	CITATIONS
361	Optical and spectroscopic properties of erbium-activated modified silica glass with 1.54 μm high quantum efficiency. , 2005, , .		4
362	Low Dimensional Composite Nanomaterials: Theory and Applications. Advances in Science and Technology, 0, , .	0.2	4
363	Glass-based erbium activated micro-nano photonic structures. , 2009, , .		4
364	Analysis of Nucleotide Variations in Genes of Iron Management in Patients of Parkinson's Disease and Other Movement Disorders. Parkinson's Disease, 2011, 2011, 1-6.	1.1	4
365	Development and optical characterization of vertical tapers in SiON waveguides using gray-scale lithography. Proceedings of SPIE, 2011, , .	0.8	4
366	Thermal Decomposition of Silicon-rich Oxides Deposited by the LPCVD Method. Croatica Chemica Acta, 2012, , 91-96.	0.4	4
367	Rare-earth phosphors for the control of WLED's colour output: State of the art. , 2014, , .		4
368	Photonic glass-ceramics: consolidated outcomes and prospects. , 2015, , .		4
369	Photodarkening and photobleaching impact on 1030 nm fiber laser emission. Journal of Optics (United) Tj ETQq1	1_0,78431 2.2	.4 rgBT /Ov€
370	Fabrication and characterization of Er ⁺³ doped SiO ₂ /SnO ₂ glass-ceramic thin films for planar waveguide applications. IOP Conference Series: Materials Science and Engineering, 2015, 73, 012102.	0.6	4
371	Novel pumping schemes of Mid-IR photonic crystal fiber lasers for aerospace applications. , 2016, , .		4
372	Low-Threshold Coherent Emission at 1.5 µm from Fully Er3+ Doped Monolithic 1D Dielectric Microcavity Fabricated Using Radio Frequency Sputtering. Ceramics, 2019, 2, 74-85.	2.6	4
373	SiO2-SnO2 transparent glass-ceramics activated by rare earth ions. , 2019, , .		4
374	Absorption and luminescence spectroscopy of zinc borate glasses doped with trivalent lanthanide ions. Radiation Effects and Defects in Solids, 1995, 135, 243-246.	1.2	3
375	Optical energy transfer in rare earth doped silica gels. Radiation Effects and Defects in Solids, 1995, 135, 247-251.	1.2	3
376	Optical and spectroscopic characterization of Er/Yb-activated planar waveguides. , 2000, , .		3
377	Efficient visible up-conversion emission in Pr3+- and Er3+-doped aluminum fluorophospate glasses. , 2000, 3942, 174.		3
378	Low-temperature specific heats of porous silica xerogels of low densities. Journal of Non-Crystalline Solids, 2001, 280, 222-227.	3.1	3

#	Article	IF	CITATIONS
379	Molecular dynamics simulation of an erbium-activated titania–silica glass: Composition influence on the structural properties. The Philosophical Magazine: Physics of Condensed Matter B, Statistical Mechanics, Electronic, Optical and Magnetic Properties, 2002, 82, 681-693.	0.6	3
380	Nucleation and Crystallization of Titania Nanoparticles in Silica Titania Planar Waveguides: a Study by Low Frequency Raman Scattering. Materials Science Forum, 2004, 455-456, 520-526.	0.3	3
381	Optical spectroscopy of Er3+ and Ce3+-codoped TeO 2 -WO 3 -Na 2 O glasses. , 2004, , .		3
382	<title>Whispering gallery mode resonators for microlasers and microsensors</title> . , 2006, , .		3
383	Effect of CO 2 laser irradiation on the performances of sol-gel-derived Er3+-activated SiO 2 - ZrO 2 and SiO 2 - HfO 2 planar waveguides. , 2007, 6458, 91.		3
384	Glass Microspherical Lasers. Advances in Science and Technology, 2008, 55, 46-55.	0.2	3
385	Micro-Raman mapping of micro-gratings in Baccarat glass directly written using femtosecond laser. Proceedings of SPIE, 2008, , .	0.8	3
386	Glass-ceramics coating of silica microspheres. , 2009, , .		3
387	Micro resonator stabilization by thin film coating. , 2009, , .		3
388	Opal-Type Photonic Crystals: Fabrication and Application. Advances in Science and Technology, 0, , .	0.2	3
389	Enhanced luminescence in Er ³⁺ -doped SiO <inf>2</inf> -ZrO <inf>2</inf> glass ceramic waveguide. , 2011, , .		3
390	Soda-zinc-aluminosilicate glasses doped with Tb3+, Ce3+, and Sm3+for frequency conversion and white light generation. , 2011, , .		3
391	Rare-earth-activated glasses for solar energy conversion. , 2011, , .		3
392	Low Temperature Deposition of SiNx Thin Films by the LPCVD Method. Croatica Chemica Acta, 0, , 97-100.	0.4	3
393	Glass-ceramics for photonics: Advances and perspectives. , 2014, , .		3
394	Tailoring the Structure and Luminescence of Nanostructured Er ³⁺ and Er ³⁺ /Yb ³⁺ â€Activated Hafniaâ€Based Systems. Journal of the American Ceramic Society, 2015, 98, 3136-3144.	3.8	3
395	Optical properties of one-dimensional disordered multilayer photonic structures. , 2015, , .		3
396	Lasing and mode selection in erbium doped 70SiO2-30HfO2 coated microspheres. Optical Materials, 2019, 87, 98-101.	3.6	3

#	Article	IF	CITATIONS
397	SiO2-SnO2:Er3+ planar waveguides: Highly photorefractive glass-ceramics. Optical Materials: X, 2020, 7, 100056.	0.8	3
398	Active Sol-Gel Materials, Fluorescence Spectra, and Lifetimes. , 2016, , 1-43.		3
399	Luminescence of theCr3+ion in sodium β- and β''-alumina: Site selection by time-resolved fluorescence line narrowing. Physical Review B, 1994, 49, 6501-6514.	3.2	2
400	High-quality $\hat{I}\pm$ -oligothiophene films grown by supersonic seeded beams: optical, morphological, and structural characterization. , 2000, , .		2
401	A comparative study of the spectroscopic properties at 1.5 μm of erbium-activated fluoride and tellurite glasses. The Philosophical Magazine: Physics of Condensed Matter B, Statistical Mechanics, Electronic, Optical and Magnetic Properties, 2002, 82, 573-585.	0.6	2
402	Molecular dynamics simulation of an erbium-activated titania-silica glass: composition influence on the structural properties. The Philosophical Magazine: Physics of Condensed Matter B, Statistical Mechanics, Electronic, Optical and Magnetic Properties, 2002, 82, 681-693.	0.6	2
403	Inorganic nanoparticles in organic-inorganic hybrid hosts for planar waveguides. , 2002, , .		2
404	Fabrication by rf-sputtering processing of Er3+/Yb3+-codoped silica-titania planar waveguides. , 2003, , .		2
405	Erbium/Ytterbium-activated silica-titania planar and channel waveguides prepared by rf-sputtering. , 2003, , .		2
406	Structural properties and luminescence of rare-earth ions in transition-metal fluoride glasses. Philosophical Magazine, 2004, 84, 1645-1650.	1.6	2
407	Hybrid organic–inorganic films by assembling of Si–Zr-based nanobuilding blocks. Journal of the European Ceramic Society, 2005, 25, 2051-2054.	5.7	2
408	Er3+- and Tm3+-Containing Ultra-Transparent Oxyfluoride-Based Glass Ceramics for Wavelength Division Multiplexing Optical Amplifiers. Glass Physics and Chemistry, 2005, 31, 377-381.	0.7	2
409	Effect of Yb3+ concentration on Er3+ luminescence properties of sol-gelderived silica-alumina xerogels. Optoelectronics Letters, 2006, 2, 354-357.	0.8	2
410	Synthesis Improvement of Yb ³⁺ -Activated SnO ₂ Nanocrystals. Solid State Phenomena, 2007, 128, 31-40.	0.3	2
411	Nanocomposite photonic glasses and confined structures optimizing Er3+-luminescent properties. , 2007, , .		2
412	Metal nanocluster and sodalime glasses: an XPS characterization. Proceedings of SPIE, 2007, , .	0.8	2
413	Ceramization of erbium activated planar waveguides by bottom up technique. , 2007, , .		2

414 Erbium-Activated Silica-Hafnia: a Reliable Photonic System. , 2008, , .

#	Article	IF	CITATIONS
415	Design of high gain Er ³⁺ -Yb ³⁺ -Ce ³⁺ co-doped ZELA fluoride glass waveguide amplifier. Proceedings of SPIE, 2008, , .	0.8	2
416	SiO 2 -SnO 2 glass-ceramic planar waveguides activated by rare earth ions. , 2009, , .		2
417	Er3+-activated photonic structures fabricated by sol-gel and rf-sputtering techniques. , 2009, , .		2
418	XPS Study of <i>In Situ</i> One-Step Amination of Nanocrystalline Diamond Films. Advances in Science and Technology, 2010, 71, 45-49.	0.2	2
419	The optical study of nanoporous C-Pd thin films. Proceedings of SPIE, 2011, , .	0.8	2
420	Down-converter based on rare earth doped fluoride glass to improve Si-based solar cell efficiency. Proceedings of SPIE, 2011, , .	0.8	2
421	Design of rare-earth doped chalcogenide microspheres for mid-IR optical amplification. Proceedings of SPIE, 2012, , .	0.8	2
422	Preface: Photoluminescence in rare earths: Photonic materials and devices. Optical Materials, 2013, 35, 1877-1878.	3.6	2
423	A parallel computational FDTD approach to the analysis of the light scattering from an opal photonic crystal. Proceedings of SPIE, 2013, , .	0.8	2
424	Rare earths and metal nanoparticles in silicate glass-ceramics to improve the efficiency of photovoltaic solar cells. , 2014, , .		2
425	Rare-earth doped optical fibers with nano-phase glass-ceramic structures. , 2016, , .		2
426	Recent advances on pumping schemes for mid-IR PCF lasers. , 2017, , .		2
427	Glass and glass-ceramic photonic systems. , 2017, , .		2
428	Finite difference analysis and experimental validation of 3D photonic crystals for structural health monitoring. , 2017, , .		2
429	Light management in solar cells: Recent advances. , 2017, , .		2
430	Analytical modelling of Tm-doped tellurite glass including cross-relaxation process. Optical Materials, 2019, 87, 29-34.	3.6	2
431	Optical spectroscopy of Eu3+ doped zinc borate glasses. European Physical Journal Special Topics, 1994, 04, C4-477-C4-480.	0.2	2
432	Site distribution and thermalization effects in europium-doped silica glasses. European Physical Journal Special Topics, 1994, 04, C4-579-C4-582.	0.2	2

#	Article	IF	CITATIONS
433	Effect of dye on the band gap of 3D polystyrene photonic crystals. Proceedings of SPIE, 2009, , .	0.8	2
434	Rare-earth-activated glass-ceramic waveguides: ideal systems for photonics. SPIE Newsroom, 0, , .	0.1	2
435	Homogeneous and inhomogeneous broadening of theA24→T12zero-phonon transition in MgO: Cr. Physical Review B, 1982, 26, 5965-5967.	3.2	1
436	Effect of a magnetic field on single-ion-to-pair transfer in ruby. Journal of Physics C: Solid State Physics, 1984, 17, L711-L714.	1.5	1
437	Waveguided Raman and Brillouin scattering. , 2000, , .		1
438	Planar Waveguides Based on Nanocrystalline and Er ³⁺ Doped SnO ₂ . Materials Science Forum, 2002, 403, 107-110.	0.3	1
439	Modeling of Er3+-doped SiO 2 -TiO 2 planar amplifier. , 2002, , .		1
440	Photoluminescence Spectroscopy of Er3+/Yb3+ Co-Activated Silica-Alumina Monolithic Xerogels. Journal of Sol-Gel Science and Technology, 2004, 32, 267-271.	2.4	1
441	Er3+/Yb3+activated silica-hafnia planar waveguides for photonics fabricated by rf-sputtering. , 2006, 6183, 173.		1
442	Application of PVD technique to the fabrication of erbium doped ZrF 4 -based glass ceramic for optical amplification. , 2006, 6183, 369.		1
443	Characterization of highly photorefractive and active silica-germania sputtered thin films. , 2006, 6123, 124.		1
444	Homogeneous and nanocomposite rare-earth-activated glasses for photonic devices. , 2006, , .		1
445	Electron confinement effects in silver nanocluster embedded in sodalime glasses. , 2008, , .		1
446	Fabrication and Spectroscopic Properties of Glass-Based Erbium Activated Micro-Nano Photonic Structures. , 2008, , .		1
447	Preparation and characterization of ZnO particles embedded in organic-inorganic planar waveguide by sol-gel route. Proceedings of SPIE, 2008, , .	0.8	1
448	Fabrication, assessment, and application of confined structures in photonic glasses. , 2009, , .		1
449	X-ray photoelectron spectroscopy of SiO 2 -HfO 2 amorphous and glass-ceramic waveguides: a comparative study. , 2009, , .		1
450	Fabrication and characterization of confined structures for sensing and lasing applications. Proceedings of SPIE, 2010, , .	0.8	1

#	Article	IF	CITATIONS
451	Rare – Earth – Doped Silicate Glass – Ceramic Thin Films for Integrated Optical Devices. Advances in Science and Technology, 0, , .	0.2	1
452	Hybrid colloidal crystal for photonic application. , 2011, , .		1
453	Erbium-activated silica-tin oxide glass ceramics for photonic integrated circuits: fabrication, characterisation, and assessment. , 2012, , .		1
454	High quality factor dielectric multilayer structures fabricated by rf-sputtering. Proceedings of SPIE, 2012, , .	0.8	1
455	Spherical resonators coated by glass and glass-ceramic films. Proceedings of SPIE, 2012, , .	0.8	1
456	Effect of zirconia in Er ³⁺ -doped SiO <inf>2</inf> -ZrO <inf>2</inf> for planar waveguide laser. , 2012, , .		1
457	Special Section Guest Editorial: Special Section on Glass Photonics for Integrated Optics. Optical Engineering, 2014, 53, 071801.	1.0	1
458	GeO2glass ceramic planar waveguides fabricated by RF-sputtering. , 2014, , .		1
459	Optical properties of C-Pd films prepared on silica substrate studied by UV-VIS-NIR spectroscopy. Proceedings of SPIE, 2014, , .	0.8	1
460	Comparison of photodarkening in 1030nm and 1070nm Yb-doped fibre lasers. Proceedings of SPIE, 2015, ,	0.8	1
461	Glass-ceramics for photonics: Laser material processing. , 2015, , .		1
462	Phosphate-based glasses and nanostructures. , 2016, , .		1
463	Advancement of Glass-Ceramic Materials for Photonic Applications. , 2017, , 133-155.		1
464	Photoluminescence of antimony-germanate-silicate glass doped with europium ions and silver nanoparticles. , 2017, , .		1
465	Rare Earth Ions Doped Down-conversion Materials for Third Generation Photovoltaic Solar Cells. , 2017, , .		1
466	Fractional-Order Theory of Thermoelasticity. II: Quasi-Static Behavior of Bars. Journal of Engineering Mechanics - ASCE, 2018, 144, 04017165.	2.9	1
467	Modal properties of an Erbium-doped asymmetric single-mode slab waveguide in the glass-ceramics SnO2-SiO2 system. Optical Materials, 2019, 87, 90-93.	3.6	1
468	SiO2-SnO2 Photonic Glass-Ceramics. , 2019, , .		1

#	Article	IF	CITATIONS
469	Modification of the Nearâ€Infrared Spontaneous Emission in Er ³⁺ â€Activated Inverse Silica Opals. Physica Status Solidi (B): Basic Research, 2020, 257, 1900476.	1.5	1
470	Towards Integrated Nanoelectronic and Photonic Devices. , 2010, , 25-41.		1
471	DENSIFICATION PROCESS IN SILICA SOL-GEL : MONITORING BY OPTICAL AND RAMAN SPECTROSCOPY. European Physical Journal Special Topics, 1991, 01, C7-501-C7-504.	0.2	1
472	Luminescent sol–gel-derived micro and nanoparticles. , 2018, , .		1
473	Role of Ag multimers as broadband sensitizers in Tb3+/Yb3+ co-doped glass-ceramics. , 2018, , .		1
474	Aqueous And Non-Aqueous Liquids On Superhydrophobic Surfaces: Recent Developments. , 0, , 269-280.		1
475	Optical spectroscopy of Eu ³⁺ ion as a tool for the study of dehydration process in silica gels. European Physical Journal Special Topics, 1994, 04, C4-569-C4-572.	0.2	1
476	Site-selective spectroscopy of Pr3+ ions in sodium [MATH]-alumina crystals. European Physical Journal Special Topics, 1994, 04, C4-473-C4-476.	0.2	1
477	Sol–Gel-Derived SnO2-Based Photonic Systems. , 2016, , 1-19.		1
478	SiO2-SnO2:Er3+ transparent glass-ceramics: fabrication and photonic assessment. , 2018, , .		1
479	Synthesis, structure and spectroscopic assessment of luminescent GdVO4:Dy3+ and DyVO4 nanoparticles. , 2018, , .		1
480	Genetic testing in neurology exploiting next generation sequencing: state of art. Neural Regeneration Research, 2020, 15, 265.	3.0	1
481	Sequencing of Von Hippel-Lindau (VHL) Gene from Genomic DNA for Mutation Detection in Italian Patients. Electronic Journal of the International Federation of Clinical Chemistry and Laboratory Medicine, 2006, 17, 12-16.	0.7	1
482	Structure- and excitation-dependent photoluminescence of As–S:Yb3+ films. Optical Materials, 2022, 124, 111971.	3.6	1
483	Application of collector pressing method to manufacture various optically transparent oxide ceramics using SPS technique. Optical Materials, 2022, 128, 112332.	3.6	1
484	Resonant Energy Transfer in Ruby under Magnetic Field. Physica Status Solidi (B): Basic Research, 1984, 123, 659-662.	1.5	0
485	<pre><title>Rare-earth-doped HfO<formula><inf><roman>2</roman></inf></formula> nanoparticles embedded in SiO<formula><inf><roman>2</roman></inf></formula>-HfO<formula><inf><roman>2</roman></inf></formula> planar waveguides: preparation and optical, structural, and spectroscopic characterization</title>.,</pre>		0
486	2000, 2910, 10. A comparative study of the spectroscopic properties at 1.5 μm of erbium-activated fluoride and tellurite glasses. The Philosophical Magazine: Physics of Condensed Matter B, Statistical Mechanics, Electronic, Optical and Magnetic Properties, 2002, 82, 573-585.	0.6	0

#	Article	IF	CITATIONS
487	Erbium spectroscopy in photosensitive tin-doped silica glass. , 2002, , .		О
488	Enhanced spectroscopic properties at 1.5 μm in Er3+/Yb3+-activated silica-titania planar waveguides fabricated by rf-sputtering. , 2003, 4829, 87.		0
489	Introduction to Nanotechnology. Charles P. Poole, Jr., and Frank J. Owens. Hoboken, NJ: John Wiley & Sons, 2003, 400 pp., \$79.95, hardcover. ISBN 0-471-07935-9 Clinical Chemistry, 2004, 50, 981-981.	3.2	Ο
490	Nonradiative relaxation rate modification by chlorine codoping of rare earth activated PZG fluoride glasses. , 2004, , .		0
491	Spectroscopic properties of Er3+-activated Ag-exchanged silicate and phosphate glasses. , 2005, , .		0
492	Optical and spectroscopic properties of a new erbium-doped soda-lime-alumino-silicate glass for integrated optical amplifiers. , 2006, , .		0
493	Raman scattering technique in characterization of glasses containing nanoparticles for integrated optoelectronics. , 2006, 6183, 163.		0
494	Nanocomposite Photonic Glasses, Waveguiding Glass Ceramics and Confined Structures Tailoring Er3+ Spectroscopic Properties. , 2007, , .		0
495	Tailoring Er ³⁺ spectroscopic properties by nanocomposite photonic glasses and confined structures. , 2007, , .		0
496	Assessment of nanocomposite photonic systems with the X-ray photoelectron spectroscopy. Optoelectronics Letters, 2007, 3, 192-194.	0.8	0
497	About nanometer sized analogues of basic electronic and optical components. , 2008, , .		0
498	Rare earth doped fluoride glass ceramics: Fabrication of waveguides by PVD and application. , 2009, , .		0
499	Design of erbium-doped microsphere lasers. Proceedings of SPIE, 2009, , .	0.8	0
500	Low loss tin silica glass ceramic waveguides doped by rare earth elaborated by sol gel route. , 2009, , .		0
501	Er3+-activated nanocomposite photonic glasses and confined structures. Optical Materials, 2009, 31, 1071-1074.	3.6	0
502	Noble metal nanoparticles functionalized with novel organic luminophores. , 2009, , .		0
503	Modeling of nano- and micro-spheres for sensing applications. , 2009, , .		0
504	ELECTRONIC CONFINEMENT OF SILVER NANOCLUSTERS IN Er ³⁺ -ACTIVATED SILICATE AND PHOSPHATE GLASSES. , 2009, , .		0

#	Article	IF	CITATIONS
505	Nanocrystal in Er[sup 3+]-doped SiO[sub 2]-ZrO[sub 2] Planar Waveguide with Yb[sup 3+] Sensitizer. , 2010, , .		0
506	Tellurite glasses rare-earth doped optical fibre devices: Recent progress and prospects. , 2010, , .		0
507	Preparation and characterization of SiO <inf>2</inf> -ZrO <inf>2</inf> :Er ³⁺ /Yb ³⁺ planar waveguides for optical amplifier. , 2010, , .		0
508	Characterisation of thin LPCVD silicon-rich oxide films. Proceedings of SPIE, 2011, , .	0.8	0
509	Tailoring the optical properties by colloidal systems. , 2012, , .		0
510	Whispering gallery modes in coated silica microspheres. Proceedings of SPIE, 2012, , .	0.8	0
511	Low-Loss Erbium Activated Silica-Tin Oxide Planar Waveguides. , 2012, , .		0
512	Glass-Based Sub-Wavelength Photonic Structures. , 2013, , .		0
513	Design of rare-earth doped microspheres lasers. , 2013, , .		0
514	Tailored spectroscopic and optical properties in rare earth-activated glass-ceramics planar waveguides. , 2013, , .		0
515	Red photonic glasses and confined structures. Bulletin of the Polish Academy of Sciences: Technical Sciences, 2014, 62, 647-653.	0.8	0
516	RF-sputtering derived dielectric 1-D photonic crystal activated with Er3+ ions. , 2014, , .		0
517	Glass-Based Photonic Crystals: From Fabrication to Applications. Advances in Science and Technology, 0, , .	0.2	0
518	Coated spherical microresonators for cutting-edge photonics application. , 2014, , .		0
519	Fiber coupled erbium doped microsphere: NIR and mid-IR wavelength ranges. , 2014, , .		0
520	Enhancing photovoltaic performance of silicon solar cells by rare earth doped glass ceramic. , 2015, , .		0
521	Strain-sensitive photonic crystals for sensing applications in structural health monitoring. , 2015, , .		0
522	Tb3+/Yb3+ Activated Silica-Hafnia Glass and Glass Ceramics to Improve the Efficiency of Photovoltaic Solar Cells. Lecture Notes in Electrical Engineering, 2016, , 475-482.	0.4	0

#	Article	IF	CITATIONS
523	RF-sputtering derived phosphosilicate planar waveguides activated by Er3+ions. , 2016, , .		0
524	Photonic crystal slab strain sensors: A viable tool for structural health monitoring. , 2016, , .		0
525	Femtosecond laser written photonic circuits in diamond for quantum information. , 2016, , .		0
526	Effect of increasing temperature on the physical properties of nano-composite phospho-silicate. , 2016, , .		0
527	Tailoring the optical properties of one-dimensional (1D) photonic structures. , 2017, , .		0
528	Bulk diamond optical waveguides fabricated by focused femtosecond laser pulses. , 2017, , .		0
529	Pulsed Bessel beam-induced high aspect ratio microstructures on diamond substrate for microfluidics and biosensing applications. , 2017, , .		0
530	Femtosecond laser processing for single NV-waveguide integration in diamond. , 2017, , .		0
531	Effect of Modifiers on Optical and Structural Properties of Barium Gallo-Germanate Glasses Doped with RE lons. , 2018, , .		Ο
532	Sol-Gel-Derived SnO2-Based Photonic Systems. , 2018, , 2301-2319.		0
533	Lasing in Er ³⁺ doped microspheres. , 2018, , .		0
534	Tungsten oxide films by radio-frequency magnetron sputtering for near-infrared photonics. Optical Materials: X, 2021, 12, 100093.	0.8	0
535	Optical Microspherical Resonators for Biomedical Applications. , 2010, , .		Ο
536	Nonlinear enhancement in 1-D photonic crystal with ZnO defect fabricated by rf sputtering. , 2012, , .		0
537	Whispering gallery mode resonators coated with active layers. , 2012, , .		0
538	Fabrication and Spectroscopic Assessment of Glass-Based Sub-Wavelength Structures for Hybrid 1-D Dielectric 633-nm Laser Microcavity. , 2014, , .		0
539	CdSxSe1-x NANOCRYSTALLITES : NEW MATERIALS FOR NON LINEAR OPTICS. European Physical Journal Special Topics, 1991, 01, C7-435-C7-437.	0.2	0
540	Glass-based confined structures enabling light control. AIP Conference Proceedings, 2015, , .	0.4	0

#	Article	IF	CITATIONS
541	Mechanochromic Photonic Crystals for Structural Health Monitoring. , 0, , .		0
542	Enhancing the absorption cross section of rare earth by silver metallic nanoparticles. , 2017, , .		0
543	Glass based structures fabricated by rf-sputtering. , 2017, , .		Ο
544	Femtosecond laser written diamond photonics. , 2018, , .		0
545	Active Sol-Gel Materials, Fluorescence Spectra, and Lifetimes. , 2018, , 1607-1649.		0
546	Energy transfer and multicolor emission in germanate glasses containing Ce3+ and Pr3+ for white light-emitting diodes. , 2018, , .		0
547	Lasing properties of Er3+ activated SiO2-HfO2 coated microspheres. , 2018, , .		0
548	Spectroscopic properties of rare earth doped germanate glasses. , 2018, , .		0
549	One-dimensional disordered photonic structures with two or more materials. , 2018, , .		0
550	Glass photonic structures fabricated by sol-gel route. , 2018, , .		0
551	Near-infrared emission in barium gallo-germanate glasses doped with Pr3+ and co-doped with Ce3+ and Pr3+ for broadband optical amplifiers. , 2018, , .		0
552	Fabrication by rf-sputtering and assessment of dielectric Er3+ doped monolithic 1-D microcavity for coherent emission at 1.5 um. , 2018, , .		0
553	Passive and active whispering gallery mode microresonators in optical engineering. , 2019, , .		Ο
554	3D-photonic crystals: Opal structures. , 2020, , 113-144.		0
555	Phoxonic glass cavities based on whispering gallery mode resonators. Optical Materials: X, 2021, 12, 100120.	0.8	0
556	Enhanced photorefractivity and rare-earth photoluminescence in SnO2 nanocrystals-based photonic glass-ceramics. EPJ Web of Conferences, 2021, 255, 05001.	0.3	0
557	Comparison of energy transfer between Terbium and Ytterbium ions in glass and glass ceramic: Application in photovoltaic. Solar Energy Advances, 2022, 2, 100012.	3.0	0
558	STRUCTURE AND CRYSTALLIZATION OF FLUOROZIRCONATE GLASSES. STUDY BY THE FLUORESCENCE OF Pr3+IONS. Journal De Physique Colloque, 1987, 48, C7-463-C7-465.	0.2	0

#	Article	IF	CITATIONS
559	FAST LASER SPECTROSCOPY FOR DETERMINATION OF ENERGY TRANSFER ON THE FRACTAL STRUCTURE OF SILICA-GELS. Journal De Physique Colloque, 1987, 48, C7-529-C7-531.	0.2	0
560	SPATIAL ENERGY TRANSFER IN MgO : Cr3+. Journal De Physique Colloque, 1985, 46, C7-95-C7-98.	0.2	0